J Periodontal Implant Sci. 2016 Aug;46(4):220-233
http://doi.org/10.5051/jpis.2016.46.4.220
pISSN 2093-2278·eISSN 2093-2286

JPIS
Journal of Periodontal & Implant Science

Research Article

"Over-inlay" block graft and differential morphometry: a novel block graft model to study bone regeneration and host-to-graft interfaces in rats

Giulia Ghiacci,[1,2] Gallia Graiani,[1] Francesca Ravanetti,[3] Simone Lumetti,[1,*] Edoardo Manfredi,[1] Carlo Galli,[1,4] Antonio Cacchioli,[3] Guido Maria Macaluso,[1,4] Roberto Sala[2]

[1]Department of Biomedical, Biotechnological, and Translational Sciences (S.Bi.Bi.T), University of Parma Dental Medicine Unit, Parma, Italy
[2]Department of Biomedical, Biotechnological, and Translational Sciences (S.Bi.Bi.T), University of Parma General Pathology Unit, Parma, Italy
[3]Department of Veterinary Science, University of Parma, Parma, Italy
[4]Institute of Materials for Electronics and Magnetism (IMEM), Italian National Research Council (CNR), Parco Area delle Scienze, Parma, Italy

Received: Feb 29, 2016
Accepted: Jun 29, 2016

***Correspondence to**
Simone Lumetti
Department of Biomedical, Biotechnological, and Translational Sciences (S.Bi.Bi.T), Dental Medicine Unit, University of Parma, Via Gramsci 14, Parma 43126, Italy.
E-mail: simone.lumetti@unipr.it
Tel: +39-0521-903665
Fax: +39-0521-347076

ORCID
Giulia Ghiacci
http://orcid.org/0000-0003-2902-2214
Gallia Graiani
http://orcid.org/0000-0003-1926-7568
Francesca Ravanetti
http://orcid.org/0000-0001-8729-3237
Simone Lumetti
http://orcid.org/0000-0002-0826-927X

ABSTRACT

Purpose: The aim of this study was to present new a model that allows the study of the bone healing process, with an emphasis on the biological behavior of different graft-to-host interfaces. A standardized "over-inlay" surgical technique combined with a differential histomorphometric analysis is presented in order to optimize the use of critical-size calvarial defects in pre-clinical testing.
Methods: Critical-size defects were created into the parietal bone of 8 male Wistar rats. Deproteinized bovine bone (DBBM) blocks were inserted into the defects, so that part of the block was included within the calvarial thickness and part exceeded the calvarial height (an "over-inlay" graft). All animals were sacrificed at 1 or 3 months. Histomorphometric and immunohistochemical evaluation was carried out within distinct regions of interest (ROIs): the areas adjacent to the native bone (BA), the periosteal area (PA) and the central area (CA).
Results: The animals healed without complications. Differential morphometry allowed the examination of the tissue composition within distinct regions: the BA presented consistent amounts of new bone formation (NB), which increased over time (24.53%±1.26% at 1 month; 37.73%±0.39% at 3 months), thus suggesting that this area makes a substantial contribution toward NB. The PA was mainly composed of fibrous tissue (71.16%±8.06% and 78.30%±2.67%, respectively), while the CA showed high amounts of DBBM at both time points (78.30%±2.67% and 74.68%±1.07%, respectively), demonstrating a slow remodeling process. Blood vessels revealed a progressive migration from the interface with native bone toward the central area of the graft. Osterix-positive cells observed at 1 month within the PA suggested that the periosteum was a source of osteoprogenitor elements. Alkaline phosphatase data on matrix deposition confirmed this observation.

JPIS
Journal of Periodontal & Implant Science

Edoardo Manfredi
http://orcid.org/0000-0003-2718-9934
Carlo Galli
http://orcid.org/0000-0001-7476-7181
Antonio Cacchioli
http://orcid.org/0000-0003-4421-6842
Guido Maria Macaluso
http://orcid.org/0000-0003-2203-3092
Roberto Sala
http://orcid.org/0000-0003-0414-3220

Conflict of Interest
No potential conflict of interest relevant to this article was reported.

Conclusions: The present model allowed for a standardized investigation of distinct graft-to-host interfaces both at vertically augmented and inlay-augmented sites, thus possibly limiting the number of animals required for pre-clinical investigations.

Keywords: Bone regeneration; Bone transplantation; Histology; Rat; Skull; Surgical procedure

INTRODUCTION

Bone grafting procedures are widely used for the management of alveolar bone deficiencies in oral and maxillofacial surgery. The success of bone grafts depends on their clinical and histological incorporation of the grafting material into the recipient site. The achievement of this goal depends on complex biological interactions occurring at the graft-host interfaces, which eventually lead to new bone formation and graft remodeling [1]. Native bone marrow and periosteum play an essential role in this process by providing the grafted area with osteogenic elements and a vascular supply. Many authors have shown that bone marrow contains a population of pluripotent mesenchymal stem cells, able to commit into bone-forming elements [2-4]. Pluripotent mesenchymal cells from the inner layer of periosteum may also migrate to the grafted area and participate in forming a basophilic collagen matrix, which is progressively vascularized and substituted with new bone [5,6]. It has been clinically demonstrated that the preservation of the periosteum or the use of a periosteal graft significantly improves bone graft incorporation and remodeling [7]. The composition of repair tissue and the rate of its ingrowth may differ depending on factors such as the morphology of the defect, the graft type, and the mechanical stability of the wound. In particular, the grafting technique may substantially influence the graft-host interface and thus the biological process of osseointegration.

The study of bone regeneration and repair often entails the use of *in vivo* models, and rat calvaria is one of the most commonly used pre-clinical settings for the testing of bone graft biomaterials, because it is relatively cheap and offers favorable anatomical access and surgical handling [8]. Both inlay and onlay grafting techniques have been tested in this animal model: inlay grafts are usually placed in retentive recipient sites, such as the cavity between two surgical bone sections, while onlay grafts are apposed to the surface of the recipient bone. Both inlay and onlay bone grafting techniques have been employed in rat calvarial bone [9]. Inlay grafts are better tested within a "critical-size" defect, defined as "the smallest intrabony wound which does not undergo spontaneous healing during the lifetime of the animal" and usually created in the parietal and/or occipital bone [10,11]. Inlay grafts represent a favorable environment for angiogenesis and osteogenic cell mobilization, as they lie in direct contact with the native bone marrow of the recipient site; however, by definition, inlay grafts cannot be performed in non-containing defects. Onlay grafts are usually fixed on the top of the cranium, although their stabilization may sometimes be difficult; the use of barrier membranes for graft fixation has been suggested for the stabilization of particulated onlay grafts [12]. However, membranes impede blood vessels and cell ingrowth from periosteum from participating in bone graft incorporation and remodeling [13].

Although native host bone and periosteum have been considered key factors for graft osseointegration [14], an animal model allowing a description of standardized graft-to-host interfaces has not been clearly documented.

http://doi.org/10.5051/jpis.2016.46.4.220

JPIS Journal of Periodontal & Implant Science

We investigated a novel block graft model presenting with both inlay and onlay features and permitting a differential morphometric analysis of graft-to host interfaces within the same surgical site of a rat calvaria. This may eventually lead to improvements in the development of complete data sets and to reductions in the number of animals required for pre-clinical testing.

MATERIALS AND METHODS

Animals

The study protocol was in accordance with EU Directive 2010/63/EU and was approved by the local Ethics Committee for Animal Testing of the University of Parma. Based on the concept of replacement, reduction, and refinement of animal studies (the 3R principle) [15], the rat was chosen as a model so as to avoid the use of higher animals and the sample size was minimized in accordance with the aims of testing the feasibility of a novel methodology and providing proof of principle with a wide range of potential applications. The sample size was calculated with an a priori power analysis with G*Power version 3.1.9.2 (Heinrich-Heine-Universität-Düsseldorf, Düsseldorf, Germany) [16], assuming a generic interindividual variability, a level of significance α=0.05 and error β=0.20 (power 1-β=0.80). As a default for a large effect size, the software suggested a value of 1.5. However, out of ethical concerns for reducing the number of animals required, we re-determined the sample size during the workflow based on new bone formation values, which were obtained progressively within lateral areas adjacent to native host bone and the periosteal area. We stopped enrolling animals in our study when the new effect size was sufficient to provide a statistical power of at least 0.8. With 4 rats enrolled in the study at 1 month we reached an effect size of 3.08, which provided us with a sample size indication of exactly 4, considering a two-tailed t-test. Standing by these results, the same number of animals was enrolled in the 3-month group.

Eight male, 4-month-old Wistar rats were therefore included in the study. During the whole experimental period the rats were kept in a monitored environment (21°C; 12:12 light cycle) and received a solid diet and water *ad libitum*.

Surgical procedures

Fifteen minutes prior to the surgical procedure, all animals received a single intra-muscular inoculation of enrofloxacin (10 mg/kg Baytril, Bayer, Leverkusen, Germany). The animals were anesthetized with an intraperitoneal injection of tiletamine hydrochloride zolazepam hydrochloride (60 mg/kg Zoletil 100, Virbac, Carros, France). The surgical site in the parietal region of the calvaria was shaved off and disinfected with povidone-iodine 10%. A midline incision from the bipupillar line to the occipital process was performed. After skin elevation, the subcutaneous fascia was incised and the calvarial bone surface was exposed by a blunt dissection through the periosteum. Particular attention was paid to maintaining the integrity of the periosteum. One full-thickness critical-size defect was created into the left parietal bone of each animal by means of a trephine burr of 5.0-mm external diameter (Biomet 3i, Palm Beach Gardens, FL, USA), under abundant irrigation with sterile saline. Discs of deproteinized bovine bone measuring 5 mm in diameter and 1.5 mm in height were placed into the defects so that the upper part of the disc exceeded the external cortical bone (Figure 1A and B). The part of the graft included within the calvarial bone thickness represents the "inlay" component, while the exceeding part represents the "over" component. A first-layer suture was applied in order to fix the periosteum, then a secondary layer of subcutaneous suture was applied to allow primary intention wound healing (Vycril 5-0, Ethicon,

http://doi.org/10.5051/jpis.2016.46.4.220

JPIS
Journal of Periodontal & Implant Science

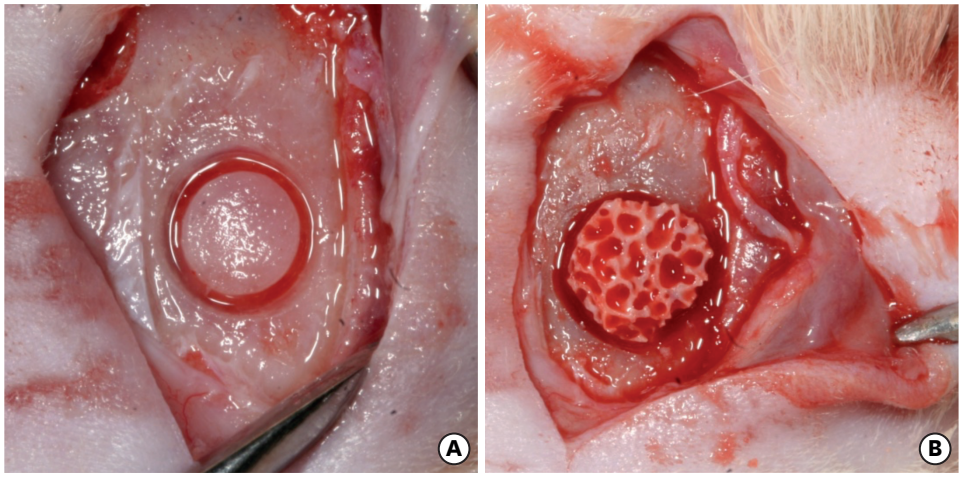

Figure 1. Surgical procedure for "over-inlay" grafting. (A) Osteotomy on parietal bone created by means of a trephine bur with a 5-mm external diameter (B) Filling of the defects with a cylindrical block graft which partially exceeded calvarial height. Optical camera (Nikon D3x, 24.5 megapixels).

Johnson&Johnson, Amersfoort, the Netherlands; Prolene 3-0, Ethicon, Johnson&Johnson, Amersfoort, the Netherlands). Care was taken not to apply the two layers of suture over the surgical defects, in order to avoid scar tissue formation within the grafted sites. All surgical operations were performed by the same trained operator. Half of the animals were sacrificed at 1 month and the remaining animals at 3 months. Euthanasia was obtained with an intraperitoneal injection of pentobarbital 150 mg/kg.

Sample processing

A partial thickness incision was performed at the surgical site, taking care not to remove periosteum. A rectangular biopsy containing the original surgical defect area and the surrounding tissues was harvested. Specimens were fixed in 10% buffered formalin for 48 hours, washed in running water, decalcified in a 0.5 M ethylene-diamine-tetra-acetic acid (EDTA) solution pH 7.4 and paraffin embedded. For each sample, serial longitudinal 5-µm-thin serial sections were cut with a rotative microtome in a plane parallel to the sagittal suture. Central sections were stained with hematoxylin-eosin for histomorphometric evaluation.

Histomorphometric analysis

The part of the grafted DBBM discs that exceeded the height of the cortical bone (the "over" component) was measured on the central vertical axis of the histological section. Calvarial thickness was also measured at the margins of the defects by tracing a vertical line connecting the external part of the inner and outer cortical bone.

Different ROIs to be analyzed were identified and respectively defined as: the periosteal area (PA), delimited on the upper part by the external periosteum and on the lower part by a straight line traced between the margins of external cortical bone of the defect; the lateral areas adjacent to native host bone (BA), described as rectangular areas extending from native bone towards the center of the defect; and the central area of the defect (CA), defined as a rectangular area traced at the remaining central portion of the defect (Figure 2A-D). Microphotographs of tissue from different ROIs were captured by an optical microscope (Nikon Eclipse 90i, Nikon, Tokyo, Japan) connected to a digital camera and morphometric

http://doi.org/10.5051/jpis.2016.46.4.220

JPIS
Journal of Periodontal & Implant Science

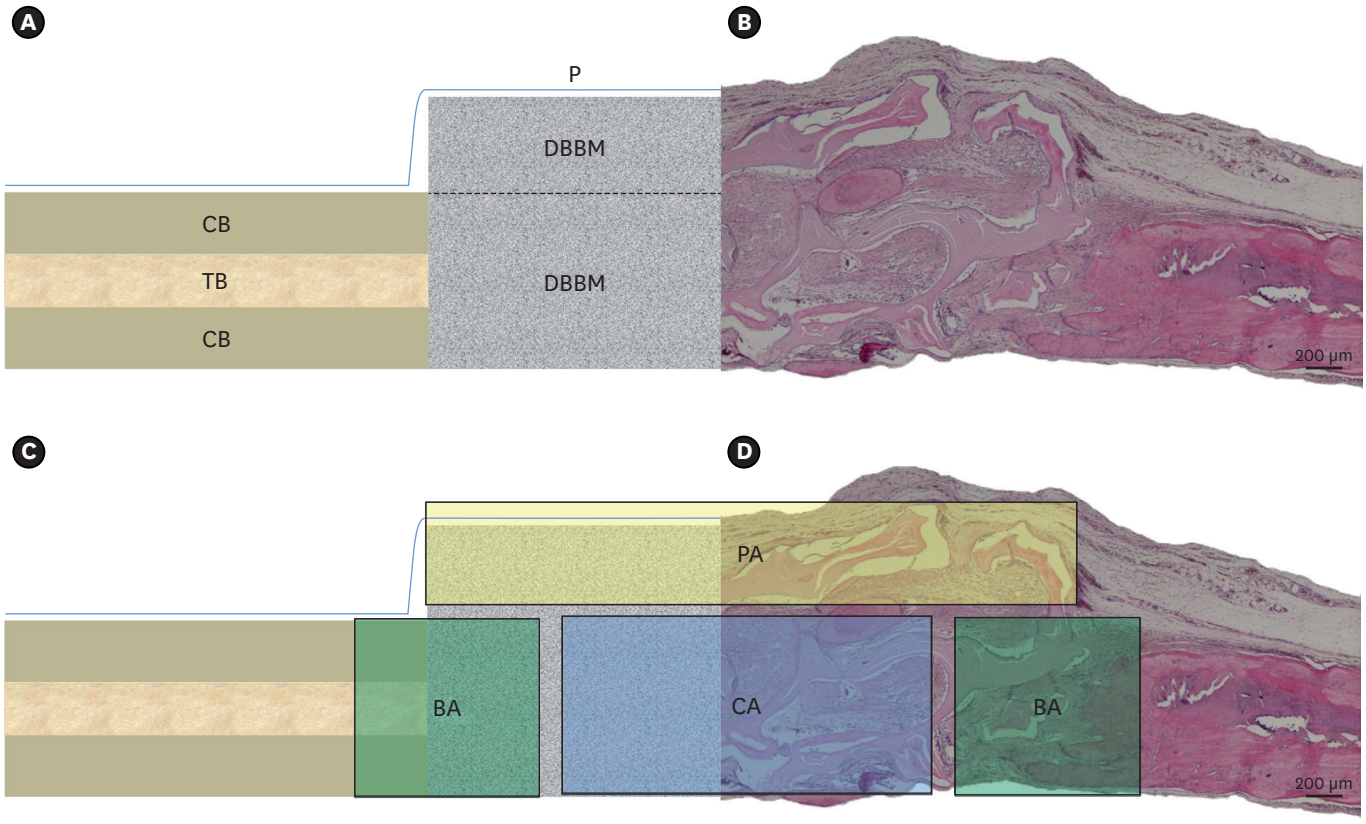

Figure 2. (A) Scheme of "over-inlay" graft and surrounding host tissues in a sagittal section: grafting material (DBBM), host trabecular bone (TB), host periosteum (P), host cortical bone (CB). Dotted line: distinction between "over" and "inlay" component of the graft. (B) Histological specimen stained with hematoxylin-eosin, showing the typical aspect of "over-inlay" graft. Optical microscopy, original magnification, 2×. (C) Scheme of regions of interest (ROIs) considered for differential histomorphometric and immunohistochemical evaluation: periosteal area (PA), lateral areas adjacent to native host bone (BA), and central area of the defect (CA). New bone formation (NB), fibrous tissue (FT), and residual deproteinized bovine bone (DBBM) were quantified within each of these ROIs, as well as alkaline phosphatase (Alp) and osterix (Osx) expression. (D) Histological specimen stained with hematoxylin-eosin, showing PA, BA, and CA ROIs considered for histomorphometric evaluation. Optical microscopy, original magnification, 2×.

evaluation of new bone formation (NB), fibrous tissue (FT), and deproteinized bovine bone (DBBM) was carried out as described elsewhere [17] by image analysis software (Image Pro-Plus 4.0, Media Cybernetics, Rockville, MD, USA) within each ROI.

Immunohistochemistry

The immunohistochemical analysis (IHC) was conducted with optical and fluorescent microscopy. Blood vessel density was assessed for the PA, BA and CA following IHC staining. Samples were incubated with anti–von Willebrand factor antibody (vWF, rabbit polyclonal, Dako, Glostrup, Denmark; 1:30, o.n), stained with streptavidin-conjugated peroxidase, using 3,3'-diaminobenzidine (DAB) as a chromogen, and finally counterstained with hematoxylin. Sections were examined at 1,000× magnification, taking advantage of an ocular reticle (9,604 mm^2 in area). A total of 20 fields within each ROI were analyzed in order to compute the capillary or venule numerical density/mm^2 of tissue.

Osteoblasts were evaluated, analyzing samples processed for IHC staining with an anti-osterix (Osx) antibody (rabbit polyclonal, Santa Cruz, CA, USA; 1:50 o.n), revealed by anti-rabbit secondary antibody FITC-conjugated (1:20 60' 37°C, Jackson Immunoresearch Laboratories, West Grove, PA, USA). The nuclear counterstaining was performed with

http://doi.org/10.5051/jpis.2016.46.4.220

4',6-diamidine-2-phenylindole (DAPI, 5mM, 18' RT; Sigma-Aldrich, St. Louis, MO, USA). Slides were mounted with the fluorescence mounting medium Vectashield (Vector Laboratories, Burlingame, CA, USA). Osx-positive cells were computed at 1,000× magnification by using fluorescent microscopy. Alkaline phosphatase (ALP) expression was assessed using an anti-Alp antibody (mouse monoclonal, Santa Cruz, CA, USA) revealed by anti-mouse secondary antibody FITC-conjugated (1:20 60' 37°C, Jackson Immunoresearch Laboratories, West Grove, PA, USA). Alp positivity was computed at 1,000× magnification by using fluorescent microscopy. IHC analysis was performed separately within each ROI.

Statistical analysis

The data distribution was verified with the Kolmogorov-Smirnov normality test. Accordingly, data were analyzed using 2-way ANOVA and the Tukey post test for multiple comparisons, considering a level of significance of $P \leq 0.05$. Results are reported as mean±standard error (SEM). Graphs were obtained with GraphPad Prism 6.0 software (GraphPad Software Inc., La Jolla, CA, USA).

RESULTS

Animals

All operated animals healed uneventfully. This finding indirectly revealed that the block graft did not exert a significant compression on the underlying tissues. The "onlay" graft component allowed the wound to heal by primary intention and no wound dehiscences were recorded at any time during the experimental period.

Histology

The grafts showed good integration in the recipient sites and no signs of inflammation or immune response were observed at any point. Newly formed bone was observed in strict contact with DBBM, thus confirming its biocompatibility as a grafting material. No sample presented with complete new bone regeneration up to the central area of the defect.

BA showed consistent areas of newly formed woven bone adjacent to native lamellar bone at both 1 month and 3 months, and projections of newly formed bone towards the grafted area were clearly identifiable. Numerous, big and roundish osteocytes were visible within this area, as well as abundant blood vessels.

PA presented with thick layers of fibrous tissue with abundant osteoblastic cells and blood vessels at 1 month. At 3 months, nodules of newly formed bone were also visible in strict contact with residual grafting material.

CA was mainly occupied by fibrous tissue and residual biomaterial, with poor new bone formation at both observation time points (Figure 3).

Histomorphometry

Calvarial thickness showed to be homogenous among different animals and did not significantly vary over time (1 month, 868.8±9.27 μm; 3 months, 914.4±71.36 μm, $P>0.05$). The portion of DBBM blocks exceeding the height of cortical bone was 43.73%±2.96% of total disc height. This indicates that a suture without tension can be achieved in this model when the

http://doi.org/10.5051/jpis.2016.46.4.220

JPIS
Journal of Periodontal & Implant Science

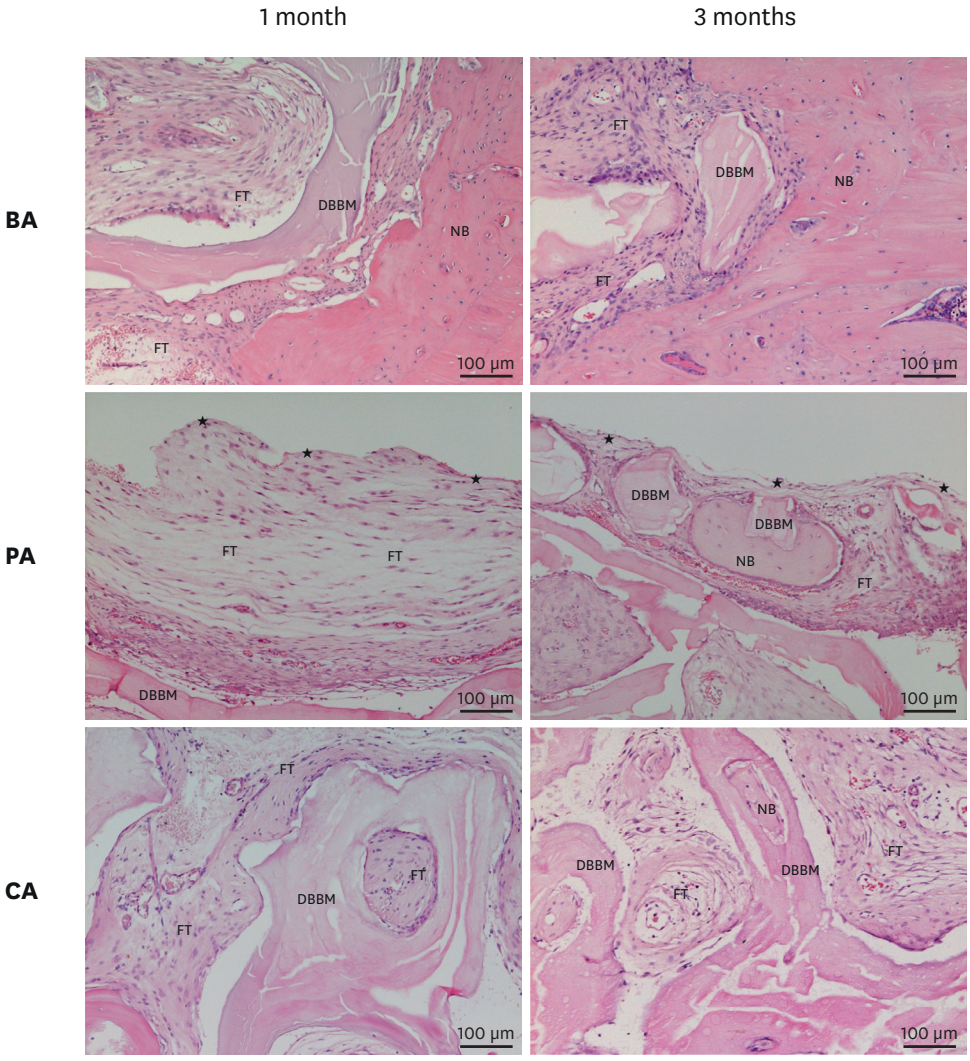

Figure 3. Representative histological details of lateral areas adjacent to native host bone (BA), periosteal areas (PA), and central areas of the defect (CA) at 1 month and 3 months of healing. Areas of new bone formation (NB), fibrous tissue (FT), and grafting material (DBBM) are marked with letters. Black stars outline periosteum level. Hematoxylin-eosin staining. Optical microscopy, original magnification, 10×.

height of the "over" component of the graft corresponds approximately to 0.4–0.7 mm.

The differential morphometric analysis applied in this study revealed differences in bone healing at distinct host-to-graft interfaces. A consistent amount of NB was observed within BA, which was found to increase from 1 month to 3 months of observation (24.53%±1.26% to 37.73%±0.39%, $P<0.05$), showing mineral apposition from native bone margins to continue over time. Also, the resulting interaction term between the two factors (tissue and observation time) was statistically significant ($P<0.05$) within BA, thus confirming the key role played by this ROI in the centripetal bone apposition process.

FT and DBBM were also observed within BA, with DBBM showing a tendency to be resorbed during the experimental period (FT, 44.90%±2.21% at 1 month, 38.24%±3.09% at 3 months, $P>0.05$; DBBM, 30.57%±3.33% at 1 month, 24.03%±3.29% at 3 months, $P>0.05$).

http://doi.org/10.5051/jpis.2016.46.4.220

JPIS Journal of Periodontal & Implant Science

PA was mainly composed of FT at both 1 month (71.16%±8.06%) and 3 months (73.14%±3.13%), without significant variations over time. At both observation time points, FT was significantly more abundant than NB (P<0.001) and DBBM (P<0.001).

Residual DBBM was the most represented tissue within CA at 1 month (78.30%±2.67%) and 3 months (74.68%±1.07%), being significantly higher than NB (P<0.001) and FT (P<0.001).

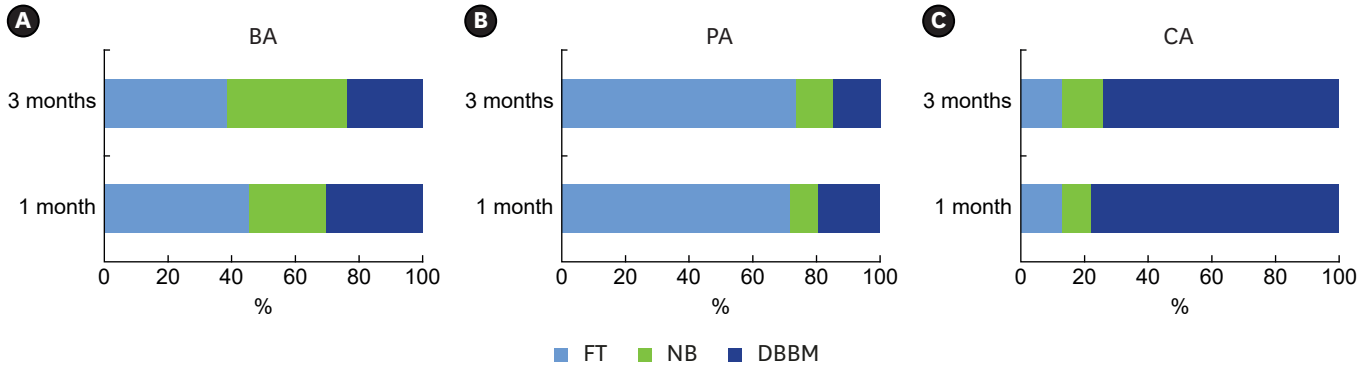

Figure 4. (A-C) New bone (NB), fibrous tissue (FT), and deproteinized bovine bone (DBBM) within lateral areas adjacent to native host bone (BA) (A), periosteal areas (PA) (B), and central area of the defect (CA) (C) at 1 and 3 months of healing. Results are expressed as mean percentages/regions of interest (ROIs).

Table 1. New bone (NB), fibrous tissue (FT), and deproteinized bovine bone (DBBM) within lateral areas adjacent to native host bone (BA) at 1 month and 3 months of healing

Parameters	1 month (n=4)		3 months (n=4)		Multiple comparisons (1 month vs. 3 months)
	mean	SEM	mean	SEM	*P*-value
NB	24.53	1.26	37.73	0.39	P<0.05
FT	44.90	2.21	38.24	3.09	NS
DBBM	30.57	3.33	24.03	3.29	NS

Data are expressed as mean percentage (%)±standard error (SEM). Multiple comparisons across time (1 month vs. 3 months) and tissue composition (NB vs. FT vs. DBBM) are also reported. *P*-value: NB vs. FT, P<0.001; NB vs. DBBM, NS; FT vs. DBBM, P<0.01; NB vs. FT, NS; NB vs. DBBM, P<0.05; FT vs. DBBM, P<0.01. Statistical significance is reported at P<0.05.

NS, not significant.

Table 2. New bone (NB), fibrous tissue (FT), and deproteinized bovine bone (DBBM) within periosteal area (PA) at 1 month and 3 months of healing

Parameters	1 month (n=4)		3 months (n=4)		Multiple comparisons (1 month vs. 3 months)
	mean	SEM	mean	SEM	*P*-value
NB	9.04	2.89	11.54	0.67	NS
FT	71.16	8.06	73.14	3.13	NS
DBBM	19.80	6.10	15.32	2.64	NS

Data are expressed as mean percentage (%)±SEM. Multiple comparisons across time (1 month vs. 3 months) and tissue composition (NB vs. FT vs. DBBM) are also reported. *P*-value: NB vs. FT, P<0.001; NB vs. DBBM, NS; FT vs. DBBM, P<0.001; NB vs. FT, P<0.001; NB vs. DBBM, NS; FT vs. DBBM, P<0.001. Statistical significance is reported at P<0.05.

NS, not significant.

Table 3. New bone (NB), fibrous tissue (FT), and deproteinized bovine bone (DBBM) within central area (CA) at 1 and 3 months of healing

Parameters	1 month (n=4)		3 months (n=4)		Multiple comparisons (1 month vs. 3 months)
	mean	SEM	mean	SEM	*P*-value
NB	9.16	2.72	12.69	0.54	NS
FT	12.53	0.55	12.63	0.53	NS
DBBM	78.30	2.67	74.68	1.07	NS

Data are expressed as mean percentage (%)±standard error (SEM). Multiple comparison across time (1 month vs. 3 months) and tissue composition (NB vs. FT vs. DBBM) are also reported. *P*-value: NB vs. FT, NS; NB vs. DBBM, P<0.001; FT vs. DBBM, P<0.001; NB vs. FT, NS; NB vs. DBBM, P<0.001; FT vs. DBBM, P<0.001. Statistical significance is reported at P<0.05.

NS, not significant.

http://doi.org/10.5051/jpis.2016.46.4.220

Indeed, NB and FT were overall poorly represented within CA at both observation time points. The interaction term between the two factors (tissue and observation time) was not significant, neither within PA nor within CA (P>0.05). Results are reported in Figure 4A-C and Tables 1-3.

Blood vessel distribution

The presence of a rich network of new vessels was detected at the host-graft interfaces and capillary density tended to vary across the analyzed areas. At 1 month, BA had a higher capillary density (13.89±2.58 n/mm^2) than PA (11.21±1.32 n/mm^2, P>0.05) and CA (8.64±2.43 n/mm^2, P>0.05); such a finding suggests the participation of this region in the process of early graft vascularization, as new vessels developing from native bone initiate colonization of the grafted site. At 3 months, CA showed a higher capillary presence (12.16±0.42 n/mm^2) compared to other areas (PA, 10.44±2.49 n/mm^2, P>0.05; BA, 6.93±1.63 n/mm^2), albeit not statistically significant (P>0.05) (Figure 5A and B).

Taken together, these data indicate a progressive migration of the angiogenic process from lateral to central areas of the graft, which is consistent with the biological process of centripetal critical-size defect healing.

Differentiation marker distribution

Analysis of Osx distribution revealed a more abundant presence of Osx-positive cells in the PA zone when compared with other ROIs at the 1-month observation period (PA, 4.71±0.40 n/mm^2 vs. BA, 1.95±0.40 n/mm^2, P<0.01; PA, 4.71±0.40 n/mm^2 vs. CA, 2.60±0.25 n/mm^2, P<0.01).

This finding indicates that cells with osteoblastic features were present within the sub-periosteal areas and suggests that the inner layer of periosteum is an important source of osteoprogenitor elements. Overall cellularity decreased by the 3-month observation period, in agreement with a more mature tissue pattern, with no significant differences observed between regions (BA, 0.65±0.13 n/mm^2; PA, 0.89±0.31 n/mm^2; CA, 1.50±0.24 n/mm^2) (Figure 5C and D).

The early bone matrix marker Alp was found to be expressed in abundance at 1 month, with a tendency to be higher in PA (BA, 11.31±2.21 n/mm^2; PA, 14.68±2.00 n/mm^2; CA, 10.42±1.13 n/mm^2, P>0.05). A decrease in Alp expression, albeit non-significant, was observed over time in all examined areas (BA, 6.12±1.05 n/mm^2; PA, 6.12±1.05 n/mm^2; CA, 6.63±0.99 n/mm^2, P>0.05), in accordance with the physiological maturation and stabilization of the wound (Figure 5E and F).

DISCUSSION

In this study, we proposed a modified block graft technique that combines aspects of both inlay and onlay procedures and provides extensive biological insights about graft interaction with host tissues. The over-inlay surgical technique entails a graft that is partially surrounded by native bone (the "inlay" component) and partially free of surrounding walls but covered with periosteum (the "over" component). The use of such a simplified model was aimed at facilitating data collection at different graft-to-host interfaces and the interpretation of the results; indeed, the "over" component served to define a periosteal area (PA) and aided the investigation of the relative contribution of the periosteum to graft integration, while the

http://doi.org/10.5051/jpis.2016.46.4.220

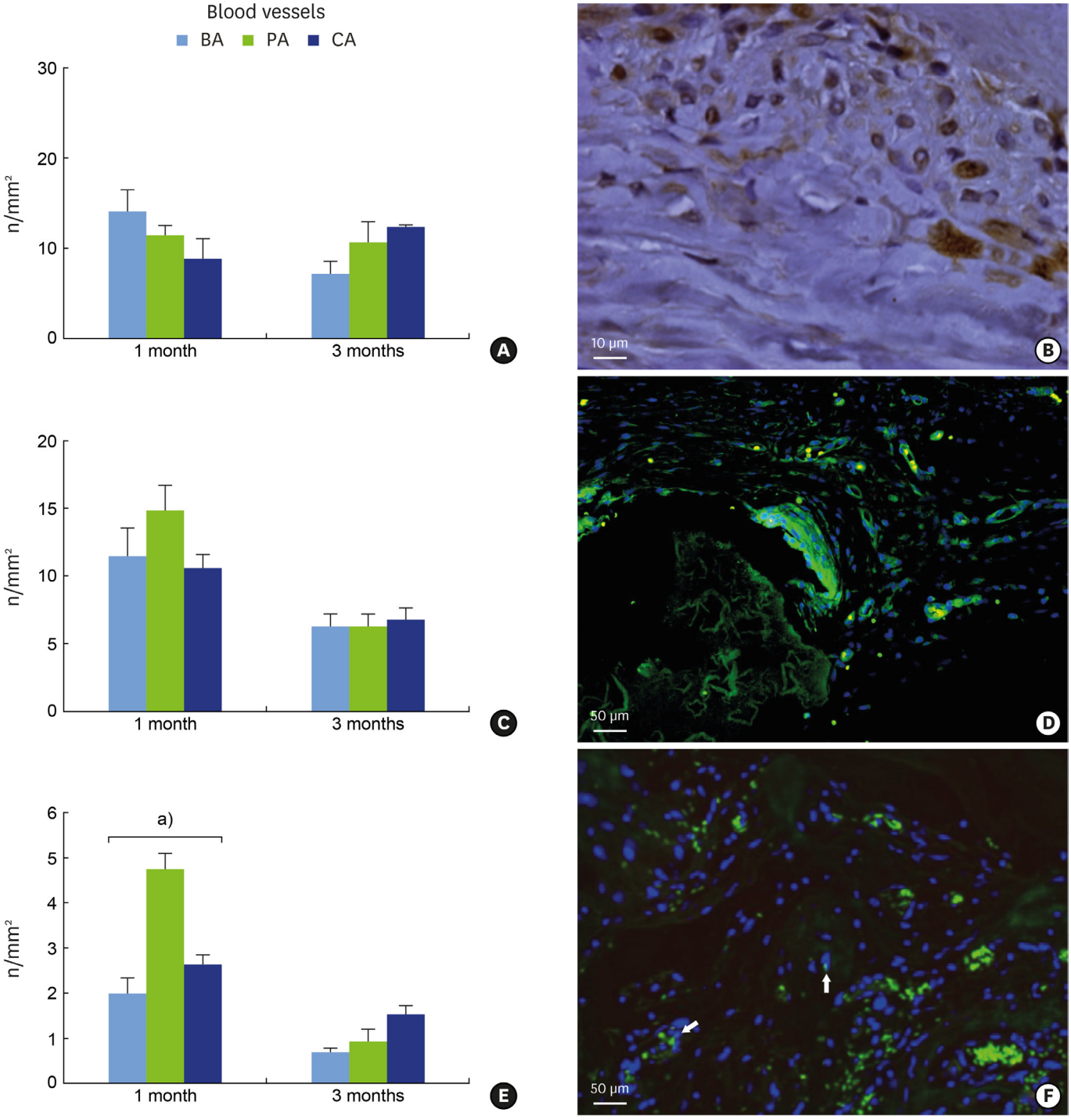

Figure 5. (A) Blood capillary density within lateral areas adjacent to native host bone (BA), periosteal areas (PA), and central area of the defect (CA) at 1 month and 3 months of healing. Results are reported as number of capillaries (n) over mm^2, mean±standard error (SEM). (B) Microscopic image showing blood vessels within PA at 1 month. Vessels are identified by brown of FVIII IHC-staining revealed by DAB. Optical microscopy, scale bar, 10 μm. (C) Density of alkaline phosphatase (Alp) positivity within lateral areas adjacent to BA, PA, and CA at 1 month and 3 months of healing. Results are reported as the number of positive elements (n) over mm^2, mean±SEM. (D) Alp positivity visualized with green fluorescence. The blue fluorescence of DAPI identifies nuclei. The image was captured within PA at 1 month. Fluorescence microscopy, scale bar, 50 μm. (E) Density of osterix (Osx)-positive cells within lateral areas adjacent to BA, PA, and CA at 1 month and 3 months of healing. Results are reported as the number of Osx-positive cells (n) over mm^2, mean±SEM. [a]Statistically significant between PA and indicated groups, $P<0.05$. (F) Osx-positive cells visualized with green fluorescence. The blue fluorescence of DAPI identifies nuclei. White arrows indicate cells with Osx-positivity. The image was captured within PA at 1 month. Fluorescence microscopy, scale bar 50 μm.

http://doi.org/10.5051/jpis.2016.46.4.220

"inlay" component allowed the study of both graft-to-native-bone interface (BA) and the central graft portion (CA).

The "over-inlay" surgical technique was adopted as a simple approach to overcome the difficulties and complications associated with the use of onlay grafts, for example, dehiscences due to excessive flap tension [18]. In our study, wounds healed by primary intention and no dehiscences were observed. The "inlay" component of the graft provided proper stabilization without the need for further fixation such as with screws that might break the graft [19] or more cumbersome procedures [20,21], whereas the "over" component was used to investigate the osteoconductive properties of the graft in the absence of the contribution from surrounding mineralized tissues or stabilizing barriers. The potential advantages of domes or membranes combined with onlay DBBM blocks have not been documented by all researchers [22,23] and the formation of a thick layer of dense connective tissue has been associated with the use of resorbable barriers [24]. Indeed, the biological importance of direct contact between the grafted area and native periosteum, which may act as a source of osteoprogenitor elements and contribute to graft osseointegration, has been extensively recognized [25,26]. By avoiding the use of barrier membranes, our model allowed for direct contact between the graft and the recipient site and thus for a differential morphometric analysis of distinct graft-to-host interfaces.

Complete bone regeneration of the surgical site was not achieved in any animal, thus confirming previous observations that pointed to 5 mm as the "critical-size" wound diameter in the calvaria of male rats between the ages of 3 and 6 months for observational periods of up to 12 months [27]. Moreover, this defect size was also compatible with the creation of bilateral defects in each parietal bone, thus allowing for split-head study designs that reduce the total number of required animals. In this study, the choice of a critical-size dimension also facilitated the histological delineation of distinct tissue apposition fronts within each ROI.

Newly formed tissues were consistently in close proximity to DBBM, which is one of the most investigated scaffolds and is widely employed in regenerative procedures, both in animal models and in clinical practice [28,29]. Many case series reported good clinical outcomes from DBBM blocks used in onlay [30,31] and inlay procedures [32,33]. Nevertheless, some authors have reported that DBBM blocks pose difficulties for the invasion of newly formed bone, which was primarily found in proximity to native medullary bone or periosteum, both in onlay [34] and inlay [35] grafts. Such findings were confirmed by our morphometric analysis of CA, which was mainly composed of residual DBBM both at 1 month and 3 months of observation. An increase in new bone formation and in the number of Osx-positive cells and blood vessels could, however, be detected within CA over time, indicating a progressive ingrowth of osteoblasts as well as a migration of the angiogenic process towards the central portion of the graft.

Native host bone appeared to make a substantial contribution to graft osseointegration, as revealed by the consistent amounts of newly formed bone and blood vessels that were noted within BA already at 1 month of observation. The role of host bone marrow has been widely emphasized as a key factor for improving graft vascularization and colonization by osteogenic elements; onlay grafts have shown better and earlier integration when the cortical bone of the recipient site was ground or perforated, thus exposing cancellous bone [36]. Previous authors who used block grafts for inlay procedures in graft calvarial critical-size defects have reported new bone at the graft borders adjacent to the host bone marrow [37] and underneath the

http://doi.org/10.5051/jpis.2016.46.4.220

periosteum [38]. In our model, a morphometric analysis of PA allowed the identification of the periosteal contribution to graft osseointegration, and a high number of Osx-positive cells and Alp positivities were found within this area. Such a result suggests that the periosteum may act as a source of osteoprogenitor elements as well as a mineralization front. This is consistent with previous reports of sub-periosteal bone formation in onlay grafts covered with native periosteum [39,40] and highlights the importance of periosteal preservation in bone regenerative procedures.

In conclusion, the "over-inlay" block graft technique provided a simple and safe surgical approach, which can be easily reproduced without risk of dehiscences. The differential histomorphometric analysis of distinct graft-to-host interfaces reflected the physiological centripetal healing of grafted critical-size defects and highlighted the contribution of different tissue compartments to graft integration.

On the whole, the novel approach presented in this study provided a deeper understanding of the biological behavior of grafts at different sites, which could facilitate the development of complete data sets when testing new biomaterials for block grafting and may lead to a reduction in the number of animals used in pre-clinical experiments.

ACKNOWLEDGEMENTS

We thank Geistlich Biomaterials, particularly Margherita Costa and Federica Bragantini, for their kind assistance and supply of materials. We thank Emilia Corradini and Gabriella Becchi (University of Parma, Italy) for technical assistance.

REFERENCES

1. Khan SN, Cammisa FP Jr, Sandhu HS, Diwan AD, Girardi FP, Lane JM. The biology of bone grafting. J Am Acad Orthop Surg 2005;13:77-86.
PUBMED | CROSSREF
2. Giuliani N, Lisignoli G, Magnani M, Racano C, Bolzoni M, Dalla Palma B, et al. New insights into osteogenic and chondrogenic differentiation of human bone marrow mesenchymal stem cells and their potential clinical applications for bone regeneration in pediatric orthopaedics. Stem Cells Int 2013;2013:312501.
PUBMED | CROSSREF
3. Wang P, Liu X, Zhao L, Weir MD, Sun J, Chen W, et al. Bone tissue engineering via human induced pluripotent, umbilical cord and bone marrow mesenchymal stem cells in rat cranium. Acta Biomater 2015;18:236-48.
PUBMED | CROSSREF
4. Liu W, Konermann A, Guo T, Jäger A, Zhang L, Jin Y. Canonical Wnt signaling differently modulates osteogenic differentiation of mesenchymal stem cells derived from bone marrow and from periodontal ligament under inflammatory conditions. Biochim Biophys Acta 2014;1840:1125-34.
PUBMED | CROSSREF
5. Colnot C, Zhang X, Knothe Tate ML. Current insights on the regenerative potential of the periosteum: molecular, cellular, and endogenous engineering approaches. J Orthop Res 2012;30:1869-78.
PUBMED | CROSSREF
6. Zhang X, Xie C, Lin AS, Ito H, Awad H, Lieberman JR, et al. Periosteal progenitor cell fate in segmental cortical bone graft transplantations: implications for functional tissue engineering. J Bone Miner Res 2005;20:2124-37.
PUBMED | CROSSREF

http://doi.org/10.5051/jpis.2016.46.4.220

7. Nagata M, Hoshina H, Li M, Arasawa M, Uematsu K, Ogawa S, et al. A clinical study of alveolar bone tissue engineering with cultured autogenous periosteal cells: coordinated activation of bone formation and resorption. Bone 2012;50:1123-9.
PUBMED | CROSSREF
8. Gomes PS, Fernandes MH. Rodent models in bone-related research: the relevance of calvarial defects in the assessment of bone regeneration strategies. Lab Anim 2011;45:14-24.
PUBMED | CROSSREF
9. Stavropoulos A, Sculean A, Bosshardt DD, Buser D, Klinge B. Pre-clinical in vivo models for the screening of bone biomaterials for oral/craniofacial indications: focus on small-animal models. Periodontol 2000 2015;68:55-65.
PUBMED | CROSSREF
10. Bosch C, Melsen B, Vargervik K. Importance of the critical-size bone defect in testing bone-regenerating materials. J Craniofac Surg 1998;9:310-6.
PUBMED | CROSSREF
11. Donos N, Lang NP, Karoussis IK, Bosshardt D, Tonetti M, Kostopoulos L. Effect of GBR in combination with deproteinized bovine bone mineral and/or enamel matrix proteins on the healing of critical-size defects. Clin Oral Implants Res 2004;15:101-11.
PUBMED | CROSSREF
12. Zigdon-Giladi H, Bick T, Morgan EF, Lewinson D, Machtei EE. Peripheral blood-derived endothelial progenitor cells enhance vertical bone formation. Clin Implant Dent Relat Res 2015;17:83-92.
PUBMED | CROSSREF
13. Hopper RA, Zhang JR, Fourasier VL, Morova-Protzner I, Protzner KF, Pang CY, et al. Effect of isolation of periosteum and dura on the healing of rabbit calvarial inlay bone grafts. Plast Reconstr Surg 2001;107:454-62.
PUBMED | CROSSREF
14. Guskuma MH, Hochuli-Vieira E, Pereira FP, Rangel-Garcia Junior I, Okamoto R, Okamoto T, et al. Bone regeneration in surgically created defects filled with autogenous bone: an epifluorescence microscopy analysis in rats. J Appl Oral Sci 2010;18:346-53.
PUBMED | CROSSREF
15. Russell WM, Burch RL. The principles of humane experimental technique. London: Methuen; 1959.
16. Faul F, Erdfelder E, Lang AG, Buchner A. G*Power 3: a flexible statistical power analysis program for the social, behavioral, and biomedical sciences. Behav Res Methods 2007;39:175-91.
PUBMED | CROSSREF
17. Cacchioli A, Ravanetti F, Soliani L, Borghetti P. Preliminary study on the mineral apposition rate in distal femoral epiphysis of New Zealand white rabbit at skeletal maturity. Anat Histol Embryol 2012;41:163-9.
PUBMED | CROSSREF
18. Fontana F, Rocchietta I, Dellavia C, Nevins M, Simion M. Biocompatibility and manageability of a new fixable bone graft for the treatment of localized bone defects: preliminary study in a dog model. Int J Periodontics Restorative Dent 2008;28:601-7.
PUBMED
19. Zecha PJ, Schortinghuis J, van der Wal JE, Nagursky H, van den Broek KC, Sauerbier S, et al. Applicability of equine hydroxyapatite collagen (eHAC) bone blocks for lateral augmentation of the alveolar crest. A histological and histomorphometric analysis in rats. Int J Oral Maxillofac Surg 2011;40:533-42.
PUBMED | CROSSREF
20. Xuan F, Lee CU, Son JS, Fang Y, Jeong SM, Choi BH. Vertical ridge augmentation using xenogenous bone blocks: a comparison between the flap and tunneling procedures. J Oral Maxillofac Surg 2014;72:1660-70.
PUBMED | CROSSREF
21. Li J, Xuan F, Choi BH, Jeong SM. Minimally invasive ridge augmentation using xenogenous bone blocks in an atrophied posterior mandible: a clinical and histological study. Implant Dent 2013;22:112-6.
PUBMED | CROSSREF
22. Rothamel D, Schwarz F, Herten M, Ferrari D, Mischkowski RA, Sager M, et al. Vertical ridge augmentation using xenogenous bone blocks: a histomorphometric study in dogs. Int J Oral Maxillofac Implants 2009;24:243-50.
PUBMED
23. De Santis E, Lang NP, Favero G, Beolchini M, Morelli F, Botticelli D. Healing at mandibular block-grafted sites. An experimental study in dogs. Clin Oral Implants Res 2015;26:516-22.
PUBMED | CROSSREF

24. Araújo MG, Sonohara M, Hayacibara R, Cardaropoli G, Lindhe J. Lateral ridge augmentation by the use of grafts comprised of autologous bone or a biomaterial. An experiment in the dog. J Clin Periodontol 2002;29:1122-31.
PUBMED | CROSSREF

25. Hoffman MD, Benoit DS. Emulating native periosteum cell population and subsequent paracrine factor production to promote tissue engineered periosteum-mediated allograft healing. Biomaterials 2015;52:426-40.
PUBMED | CROSSREF

26. Adeyemo WL, Reuther T, Bloch W, Korkmaz Y, Fischer JH, Zöller JE, et al. Influence of host periosteum and recipient bed perforation on the healing of onlay mandibular bone graft: an experimental pilot study in the sheep. Oral Maxillofac Surg 2008;12:19-28.
PUBMED | CROSSREF

27. Vajgel A, Mardas N, Farias BC, Petrie A, Cimões R, Donos N. A systematic review on the critical size defect model. Clin Oral Implants Res 2014;25:879-93.
PUBMED | CROSSREF

28. Fuegl A, Tangl S, Keibl C, Watzek G, Redl H, Gruber R. The impact of ovariectomy and hyperglycemia on graft consolidation in rat calvaria. Clin Oral Implants Res 2011;22:524-9.
PUBMED | CROSSREF

29. Milani S, Dal Pozzo L, Rasperini G, Sforza C, Dellavia C. Deproteinized bovine bone remodeling pattern in alveolar socket: a clinical immunohistological evaluation. Clin Oral Implants Res 2016;27:295-302.
PUBMED | CROSSREF

30. Steigmann M. A bovine-bone mineral block for the treatment of severe ridge deficiencies in the anterior region: a clinical case report. Int J Oral Maxillofac Implants 2008;23:123-8.
PUBMED

31. Hämmerle CH, Jung RE, Yaman D, Lang NP. Ridge augmentation by applying bioresorbable membranes and deproteinized bovine bone mineral: a report of twelve consecutive cases. Clin Oral Implants Res 2008;19:19-25.
PUBMED

32. Felice P, Marchetti C, Piattelli A, Pellegrino G, Checchi V, Worthington H, et al. Vertical ridge augmentation of the atrophic posterior mandible with interpositional block grafts: bone from the iliac crest versus bovine anorganic bone. Eur J Oral Implantology 2008;1:183-98.
PUBMED

33. Felice P, Piattelli A, Iezzi G, Degidi M, Marchetti C. Reconstruction of an atrophied posterior mandible with the inlay technique and inorganic bovine bone block: a case report. Int J Periodontics Restorative Dent 2010; 30:583-91.
PUBMED

34. Veis A, Dabarakis N, Koutrogiannis C, Barlas I, Petsa E, Romanos G. Evaluation of vertical bone regeneration using block and particulate forms of bio-oss bone graft: a histologic study in the rabbit mandible. J Oral Implantol 2015;41:e66-72.
PUBMED | CROSSREF

35. Antunes AA, Grossi-Oliveira GA, Martins-Neto EC, Almeida AL, Salata LA. Treatment of circumferential defects with osseoconductive xenografts of different porosities: a histological, histometric, resonance frequency analysis, and micro-CT study in dogs. Clin Implant Dent Relat Res 2015;17 Suppl 1:e202-20.
PUBMED | CROSSREF

36. Alberius P, Gordh M, Lindberg L, Johnell O. Onlay bone graft behaviour after marrow exposure of the recipient rat skull bone. Scand J Plast Reconstr Surg Hand Surg 1996;30:257-66.
PUBMED | CROSSREF

37. Marins LV, Cestari TM, Sottovia AD, Granjeiro JM, Taga R. Radiographic and histological study of perennial bone defect repair in rat calvaria after treatment with blocks of porous bovine organic graft material. J Appl Oral Sci 2004;12:62-9.
PUBMED | CROSSREF

38. Park JC, So SS, Jung IH, Yun JH, Choi SH, Cho KS, et al. Induction of bone formation by Escherichia coli-expressed recombinant human bone morphogenetic protein-2 using block-type macroporous biphasic calcium phosphate in orthotopic and ectopic rat models. J Periodontal Res 2011;46:682-90.
PUBMED | CROSSREF

39. Alberius P, Gordh M. Osteopontin and bone sialoprotein distribution at the bone graft recipient site. Arch Otolaryngol Head Neck Surg 1998;124:1382-6.
PUBMED | CROSSREF

40. Murata M, Huang BZ, Shibata T, Imai S, Nagai N, Arisue M. Bone augmentation by recombinant human BMP-2 and collagen on adult rat parietal bone. Int J Oral Maxillofac Surg 1999;28:232-7.
PUBMED | CROSSREF

http://doi.org/10.5051/jpis.2016.46.4.220